Naturally embedded SSVEP phase tagging in a P300-based BCI: LSC-4Q speller*

Gabriel Pires[1], Mine Yasemin[2] and Urbano J. Nunes[3]

***Abstract*— This paper proposes a P300-based BCI speller called LSC-4Q that takes advantage of steady state visual evoked potentials (SSVEP) that appear naturally in the brain as a side effect of the inter-stimulus interval of P300 visual paradigms. The LSC-4Q speller has a circular layout divided into quadrants, and symbols flash individually with a given pseudo-random strategy. Controlling the sequence of the events such that consecutive flashes alternate between sides or quadrants of the speller, we research the possibility of detecting the SSVEP phase associated with the side or quadrant for which the user is focusing on the target symbol, without explicitly incorporating a SSVEP flickering stimulator. The SSVEP phase is extracted using a statistical spatio-spectral Fisher criterion beamformer (SSFCB) implemented in the frequency domain. Results show that SSFCB efficiently extracts phase tags from the SSVEPs embedded on the visual evoked potentials of the oddball paradigm. Preliminary results with 4 participants suggest that it is possible to detect with high accuracy the side of the screen to which the user is looking, and with less precision the detection of the quadrant. Main issues are related to phase variability across sessions. Online results show that some participants can benefit from the combined P300-Lateral approach, improving the overall classification when P300 misclassifications occur.**

I. INTRODUCTION

A Brain-computer interface (BCI) provides a control channel for people with severe motor disabilities, independent of muscular activity [1]. In severe situations, such as people with amyotrophic lateral sclerosis (ALS) in complete locked-in-state (CLIS), people loose completely the ability to control movement, including vertical and horizontal eye movements [2]. In these cases, BCI has to be controlled without resorting to any muscular activity including ocular movements [3] [4]. However, CLIS cases are very rare, and people go through several phases until they reach such condition. In most cases of severe motor impairment, such as middle and advanced stages of ALS and other motor-related neurological conditions most people preserve some residual functionality (e.g., ocular movement, facial muscular activity, speech sounds, head movements, skin sensation). It is therefore important that BCIs are designed to take advantage of end-users capabilities available, for example, by combining multiple biosignal inputs or different neural mechanisms, under the concept of hybrid BCIs (hBCIs) [5]. Hybrid BCIs can not only broaden the range of end-users who can benefit from BCI technology, but also help improve BCI's throughput and reliability. Hybrid BCIs have been proposed in diverse ways, namely, combining electroencephalography (EEG) with multiple biosignals, such as electromyography and electrooculography, or integrating different types of stimulation (e.g., visual, auditory, tactile), or combining different neural mechanisms (e.g., P300 event related potentials (ERP), steady state visual evoked potentials (SSVEP) and event related synchronization/desynchronization (ERS/ERD)) [6]. In particular, P300 and SSVEP have been combined to improve communication transfer rates or as a strategy for asynchronous BCI control [7] [8] [9]. In P300-SSVEP hBCIs proposed until now, the SSVEP stimulator is explicitly based on flickering stimuli working in parallel with the P300 oddball paradigm. Here, we introduce a novel P300-based BCI system called LSC-4Q (lateral single character - 4 quadrant) speller, which extends our previous LSC speller [10] by adding phase detection of SSVEPs naturally elicited by the P300 visual stimuli. The original LSC speller is a visual P300-based BCI, in which symbols flash individually in a circular layout. LSC was already thoroughly validated with able-bodied and motor disabled subjects [10], comparing favorably over the standard row-column speller [11]. It was already used in different contexts, for example in combination with error related potentials (ErrPs) to detect and correct errors automatically [12].

In this paper, without explicitly integrating a SSVEP stimulator, we take advantage of a side effect of P300 visual paradigms, which generate a stimulation frequency related to the inter-stimulus interval of the events, thereby naturally eliciting SSVEPs. Controlling the P300 event sequence between sides and quadrants of the speller, we investigate whether it is possible to detect the screen side or even the quadrant to which the user is gazing the target symbol, through extraction of SSVEP phase. Phase coded flickering stimuli is commonly used to increase the transfer rate of SSVEP-BCIs [13], but here we try to measure the frequency and phase evoked from random spatial events in an oddball paradigm. The flashing event strategy of the P300 LSC-4Q paradigm induces phase shifts on the SSVEP which

*This work has been financially supported by the Project B-RELIABLE: SAICT/30935/2017, with FEDER/FNR/OE funding through programs CENTRO2020 and Portuguese foundation for science and technology (FCT), and by UID/EEA/00048/2013 with FEDER funding, through programs QREN and COMPETE.

[1]Gabriel Pires is with the Institute for Systems and Robotics, University of Coimbra, 3030-290, Portugal, and also with the Engineering Department of the Polytechnic Institute of Tomar, 2300-313 Tomar, Portugal gpires@isr.uc.pt

[2]Mine Yasemin is with the Institute for Systems and Robotics, University of Coimbra, 3030-290, Portugal mine.yasemin@isr.uc.pt

[3]Urbano J. Nunes is with the Institute for Systems and Robotics, University of Coimbra, 3030-290, Portugal, and also with the Department of Electrical and Computer Engineering of the University of Coimbra, 3030-290, Portugal urbano@isr.uc.pt

Fig. 1. Printscreen of LSC layout. Highlighted letter is the stimulus event.

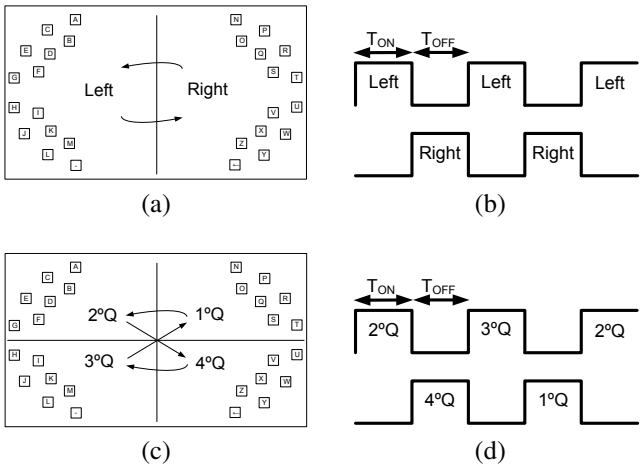

Fig. 2. a) Event sequence in LSC paradigm; b) Temporal diagram of LSC events; c) Event sequence in LSC-4Q paradigm; d) Temporal diagram of LSC-4Q events.

can be measured by a phase detection algorithm. In a previous analysis made from datasets obtained in [12] we concluded that over 30% of P300 miss-detections were from symbols in different sides and ≈ 60% in different quadrants. Therefore, the detection of sides or quadrants of the speller can contribute to improve BCI throughput and reliability. On the other hand, this paper also aims to show that different layouts and stimulation strategies of P300 visual paradigms can be used to evoke other neurophysiological characteristics that go beyond P300 ERPs.

II. METHODS

A. EEG data Acquisition

The setup of the LSC-4Q BCI consisted of a g.tec g.USBamp bioamplifier used to record EEG signals from 12 electrodes (Fz, Cz, C3, C4, CPz, Pz, P3, P4, PO7, PO8, POz and Oz) placed according to the international extended standard system. The right or left earlobe was used as reference and the AFz electrode as ground. The EEG signals were sampled at 256 Hz and filtered using a 1-60 Hz bandpass filter and a 50 Hz notch filter.

B. LSC-4Q paradigm and neurophysiological analysis

1) P300 paradigm: Fig. 1 shows a printscreen of the layout of the P300 BCI speller, which was introduced in [10]. The speller was named lateral single character (LSC) because the symbols flash individually and randomly, but consecutive flashes always alternate between left and right sides of the screen (Fig. 2a) with no inter-stimulus interval (ISI). LSC comprises all the letters of the alphabet and the 'space' and 'del' symbols (28 symbols at all). The number of rounds of each trial (N_{rep}) is usually adjusted individually to each participant according to the user's BCI performance. The inter-trial interval (ITI) is set to 4 s, giving the user enough time to shift his/her attention to the next desired symbol. The overall time for one trial is:

$$TT = N_{rep} \times N_s \times SOA + CT + ITI \quad (1)$$

where $N_s = 28$ is the number of symbols, SOA is the stimulus onset asynchrony usually set to 50 or $75ms$ and $CT = 1s$ is the time associated with the last flash of the trial. A new mode was added in which consecutive events alternate sequentially between the 4 quadrants (Fig. 2c), called LSC-4Q. The paradigm settings are exactly the same of LSC, except that flash events alternate between quadrants. The temporal diagrams of the flashing events of LSC and LSC-4Q are represented respectively in Fig. 2b and Fig. 2d.

2) SSVEP side effects: Although the ISI is 0, since the events alternate between the two sides of the screen, the user sees a virtual T_{ON}-T_{OFF} effect (virtual ISI) different from 0. Associated to the virtual ISIs perceived by the user, different SSVEPs are expected to be elicited as a side effect of the P300 paradigm, at the following frequencies:

$$f_{SSVEP} = \begin{cases} \frac{1}{T_{ON}}, & \text{for all events} \\ \frac{1}{2T_{ON}}, & \text{for events of the same side} \\ \frac{1}{4T_{ON}}, & \text{for events of the same quadrant} \end{cases} \quad (2)$$

For example, for a highlight time (T_{ON}) of 50 ms, the expected SSVEP frequency elicited from all events is 20 Hz ($1/0.05$), while for side-events is 10 Hz and for quadrant-events the frequency is 5 Hz. These frequencies are clearly visible in the frequency spectrum of Fig. 3c obtained from a representative recorded dataset. When searching for brain inter-hemispheric differences and new neurophysiological features, we found out that the 10 Hz signal suffered a phase shift of 180° in opposite EEG channels, as observed in Fig. 3a for channels PO7 and PO8. This led us to check what was being elicited by left/right events when the user was gazing targets at left vs. right side. Fig. 3b shows that the SSVEPs evoked by left events have a phase shift when the user gazes left vs. right targets. Similarly, this shift can be observed in 5 Hz SSVEP elicited in LSC-4Q mode, although not in such a strong way. The plots were obtained from the average of multiple event epochs (560 left events and 280 quadrant events of a recoded dataset of 2240 events). These results showed that a phase could be detected associated with the side or quadrant of the P300 target event. The following section describes the detection methodology.

C. P300 detection

The P300 detector uses the classification framework proposed in [14]. After preprocessing, the EEG signal is segmented into 1 s epochs, $X_{N\times T}$, where N is the number

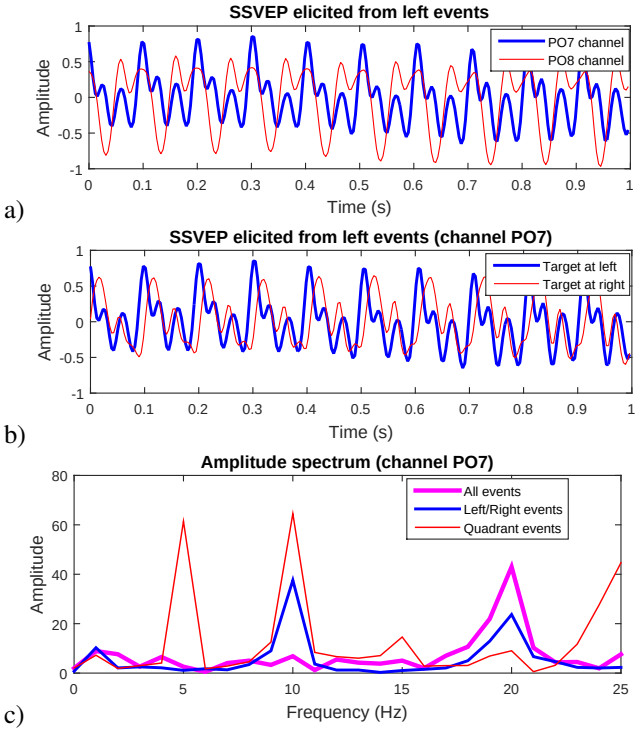

Fig. 3. Average results obtained from a dataset with 2240 epochs, considering a SOA of 50 ms. a) SSVEP recorded at channels PO7 and PO8 elicited from left events; b) SSVEP recorded at channel PO7 when user is focusing left or right target; c) Frequency spectrum taking respectively all events, left events, and quadrant events.

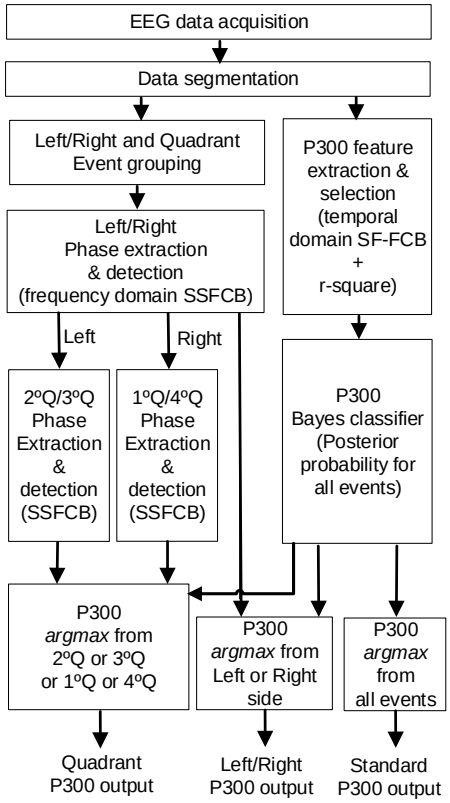

Fig. 4. Classification pipeline for the three approaches: standard P300, P300 + side detection, P300 + quadrant detection.

of channels and T is the number of time samples. The features are extracted using a statistical spatial filter based on a Fisher criterion beamformer (SF-FCB) that significantly enhances the P300 signal-to-noise ratio. The EEG epochs $X_{N\times T}$ are projected into $Y = W_p' X$, where W_p is the optimal spatial filter obtained from the calibration phase using target and non-target events, and $'$ represents the transpose operator. Features are then selected and classified with a Bayes classifier obtained from calibration (see details in [14]). Figure 4 shows the overall classification pipeline for P300 and phase detectors.

D. SSVEP-LSC-4Q phase detection

1) Epoch extraction: The SSVEP phase detector takes the EEG epochs already segmented for the P300 classifier. For Left/Right detection, the EEG epochs are grouped into left/right events according to:

- $\mathbf{X}^{ll}$: left event epochs when target is at left;
- $\mathbf{X}^{lr}$: left event epochs when target is at right;

where *l,r* superscripts refer to left and right respectively. It should be noted that the left events are used as the reference for the location of left and right P300 targets (it is always assumed that the user is gazing the target symbol). The 4-quadrant detection is implemented in two steps, left/right detection and then up/down for the detected side, i.e., 2°Q vs 3°Q and 1°Q vs 4°Q. Therefore the events are grouped into quadrant events, according to:

- $\mathbf{X}^{22}$: 2°Q event epochs when target is at 2°Q;
- $\mathbf{X}^{23}$: 2°Q event epochs when target is at 3°Q;
- $\mathbf{X}^{11}$: 1°Q event epochs when target is at 1°Q;
- $\mathbf{X}^{14}$: 1°Q event epochs when target is at 4°Q;

were the superscripts refer to the quadrants. For the left events the reference is the 2°Q events and for the right events the reference is the 1°Q events. So the classification is always binary for both LSC and LSC-4Q modes. For each of the above groups, the average of all available epochs within a trial is computed as:

$$\mathbf{X} = \frac{1}{N_{re}N_{ev}} \sum_{i=1}^{N_{rep}} \sum_{j=1}^{N_{ev}} X(i,j), \tag{3}$$

where N_{rep} is the number of event repetitions used in the P300 paradigm (selected according to user performance) and N_{ev} is the number of left events (14 events) in LSC or quadrant events (7 events) in LSC-4Q.

2) SSFCB feature extraction: The feature extractor is a frequency domain version of the statistical SF-FCB called spatio-spectral Fisher criterion beamformer (SSFCB) which is applied to the averages obtained in (3). SSFCB first obtains $\tilde{X}_{N\times F} = DFT\{X_{N\times T}\}$, where DFT stands for the Discrete Fourier Transform and F is the number of frequency bins (1 Hz resolution). The tilde symbol is used to refer to the frequency domain. The spatio-spectral projection in the frequency domain is given by

$$\tilde{\mathbf{Y}} = \tilde{W}^H \tilde{\mathbf{X}}.\tilde{\mathbf{h}} = \tilde{W}^H \tilde{\mathbf{Z}} \tag{4}$$

where $\tilde{W}$ is the spatial filter, the superscript H denotes the Hermitian transpose, and $\tilde{\mathbf{Z}}$ represents the spectrally shaped components in the frequency domain. The spectral filter is a weighting vector $\tilde{\mathbf{h}} = [\beta(1) \quad \beta(2) \quad \cdots \quad \beta(T')]$, where the coefficients β are adjusted according to the discriminative frequency bands. In its simple form, which was used here, the weights act as a mask where 1 is used for a discriminative frequency and 0 for a non-discriminative frequency. The spatial filter $\tilde{W}$ is obtained by maximizing the Rayleigh quotient

$$J(\tilde{W}) = \frac{\tilde{W}^H \tilde{\mathbf{S}}_b \tilde{W}}{\tilde{W}^H \tilde{\mathbf{S}}_w \tilde{W}}. \tag{5}$$

where matrices $\tilde{\mathbf{S}}_b$ and $\tilde{\mathbf{S}}_w$ are respectively the spatial between-class matrix and the spatial within-class matrix, computed from two classes (for example, in left/right detection, one class corresponds to left events when the user is focused on targets on the left and the other class corresponds to left events when the user is focused on targets on the right). The matrices are computed using the same expressions used in the temporal domain (see [14]). The first projection of the spatio-spectral filter is obtained in the frequency domain from

$$\tilde{\mathbf{y}} = \tilde{W}^{(1)\prime} \tilde{\mathbf{Z}}. \tag{6}$$

3) Phase identification and classification: Considering the frequency of the elicited SSVEP as f_r, then the phase shift ϕ_s of $\tilde{\mathbf{y}}(\mathbf{f})$ is obtained directly in the frequency domain from

$$\phi_s = \phi(f_r) = \angle \tilde{\mathbf{y}}(f_r) = \arctan\left(\frac{Im\{\tilde{\mathbf{y}}(f_r)\}}{Re\{\tilde{\mathbf{y}}(f_r)\}}\right). \tag{7}$$

The detected phases of every P300 round are then classified with a Bayes classifier. The class is detected using the maximum *a posteriori* decision rule

$$\hat{c} = \arg\max\{P(C_1|\phi(f_r)), P(C_2|\phi(f_r))\} \tag{8}$$

where $P(C_i|\phi(f_r))$ is the *a posteriori* probability of classes $i \in \{l, r\}$, $i \in \{2°\text{Q}, 3°\text{Q}\}$, $i \in \{1°\text{Q}, 4°\text{Q}\}$, respectively for left/right, and for $2°\text{Q}/3°\text{Q}$ and $1°\text{Q}/4°\text{Q}$ classifications. That is, the P300 target is selected from the restricted events on the side or quadrant detected.

III. Experiments and Results

A. Offline analysis

The system was validated by 4 participants. Each participant did a P300 calibration session, where they had to attend the characters 'FYNLEUP-GWQJCXRH' (16 characters) which were successively provided at the center of the screen. The calibration characters were selected to have an equal number at each quadrant. For each character all symbols were repeated 5 times ($N_{rep} = 5$). During each calibration session (about 5 min) 2240 epochs were collected (80 targets, 2160 non-targets, 1120 left and right events, and 560 events for each quadrant). These ground-truth data were used to build the classifiers for P300, left/right and quadrant detection. Two datasets were recorded, one for training and the other for testing.

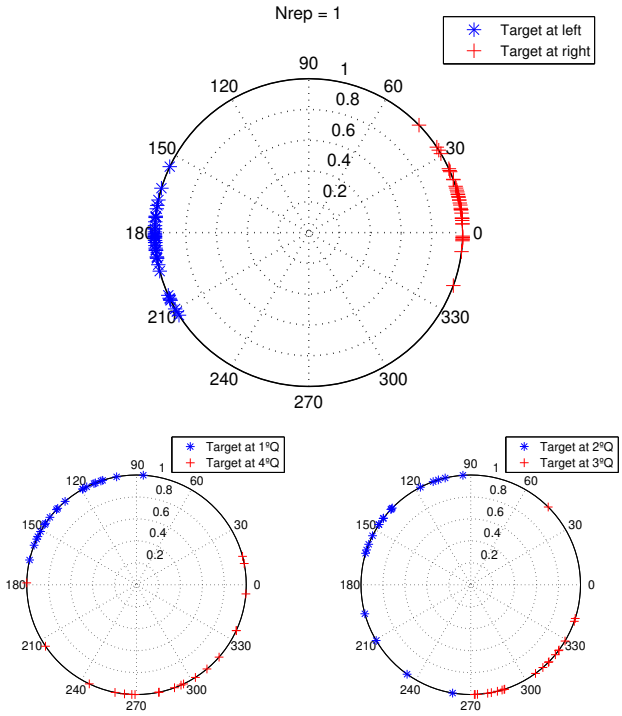

Fig. 5. Polar graphs with phases detected for $N_{rep} = 1$, discriminating left/right sides (top), and discriminating $1°\text{Q}/4°\text{Q}$ $2°\text{Q}/3°\text{Q}$ quadrants (bottom).

Applying the procedure described in section II-D, we obtained the phases detected for Left/Right sides, and the phases detected for $1°\text{Q}/4°\text{Q}$ and $2°\text{Q}/3°\text{Q}$ quadrants. Fig. 5 shows the results for one participant considering $N_{rep} = 1$. The phases detected for left/right targets show a clear phase discrimination of $\approx 180°$. The phases detected for quadrant discrimination are more disperse and the phase shift of $180°$ between left quadrants and right quadrants is not so clear. Taking the two recorded datasets during calibration, we analyzed the performance and generalization of the classification methodology. One dataset was used for training (SSFCB model and Bayesian classifier model) and the second dataset was used for testing. The classification accuracy was obtained for N_{rep} varying from 1 to 5, as shown in Fig. 7. The results show that the left/right classification accuracy is 100% for $N_{rep} = 1..5$. The quadrant classification accuracy reaches the maximum of 87% for $N_{rep} = 4$, and is higher than 75% for the remaining N_{rep}. The corresponding measured phases for $N_{rep} = 5$ were plotted in Fig. 6 to understand the variability across sessions and across participants. The first row shows the phases measured considering the same dataset1 for training and testing, while the second row shows the phases measured using dataset1 for training and dataset2 for testing. There is a difference of the mean phase across participants that can reach $30°$ and it is observed a phase inversion for participant P2. The phase difference measured for left and right targets is high, but is not always $180°$. All participants exhibit a phase shift between session1 and session2 reaching more

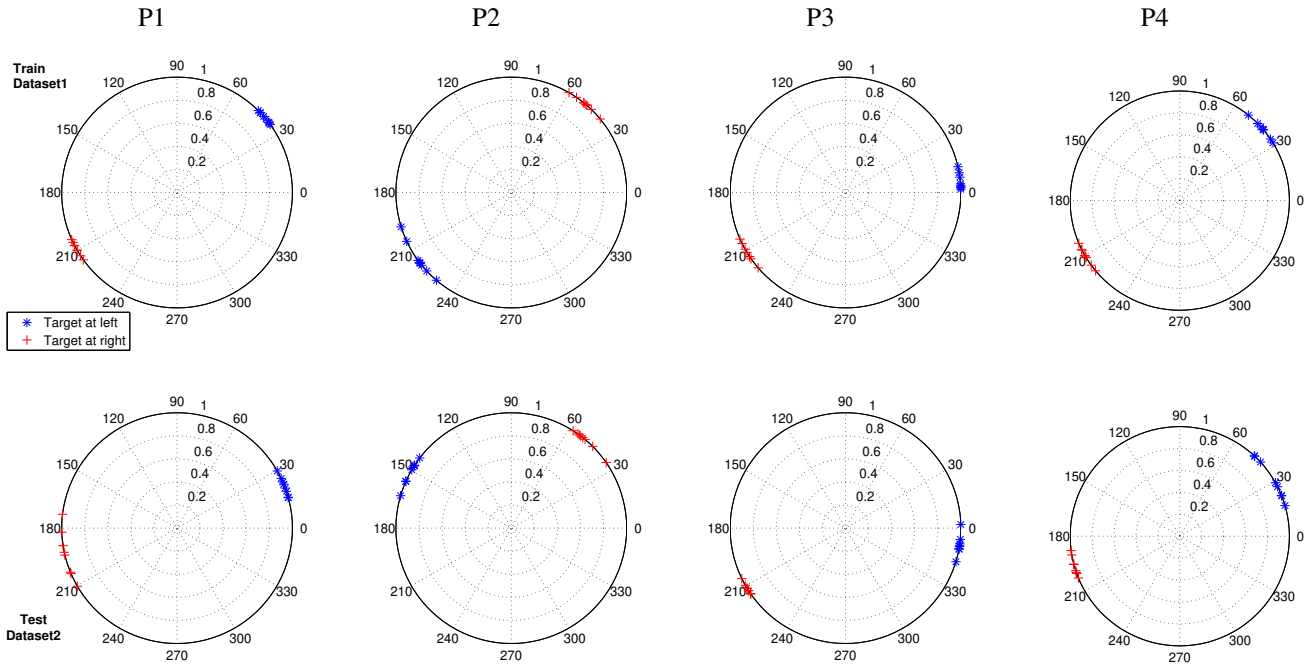

Fig. 6. Polar graphs with phases measured for left/right discrimination for the 4 participants (P1-P4). Top row shows the phases measured considering the same dataset (dataset1) for training and testing, while bottom row shows the phases measured considering dataset1 for training and dataset2 for testing. Phases were measured for $N_{rep} = 5$.

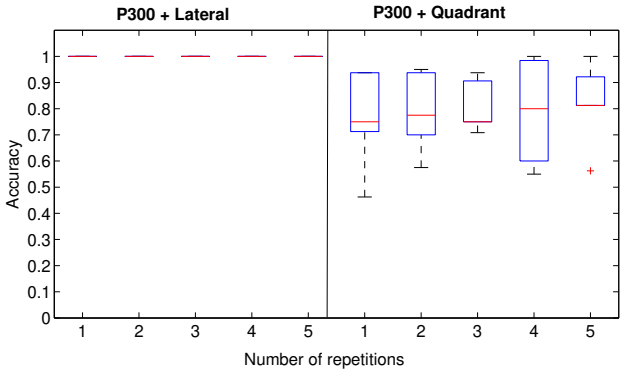

Fig. 7. Average performance for side and quadrant classification for $N_{rep} = 1..5$ (for each round of the P300 Paradigm). Results were obtained offline considering one dataset for training and a different dataset for testing.

than 30° for some participants, which may have impact on the generalization of the classifier. Although not plotted, for the quadrant detection, it was observed that the measured phases across sessions have a much higher variability than for side detection, which explains the worse accuracy in Fig. 7.

B. Online performance

The 4 participants underwent an online experiment. In the same conditions of the calibration, participants were asked to spell the 20 character sentence 'OPEN-BCI-CLOUD-WORLD', with $N_{rep} = 5$. The feedback of the detected symbols was based on the standard P300 speller (without phase detection). However, the classification algorithms for the hybrids P300-lateral and the P300-4Q were also running and the respective outputs were recorded. The results are displayed at Table I. Results show that the lateral classification is $\geq 95\%$ for 3 of the participants, but only 75% for participant P2, which was lower than expected from the offline results. Quadrant classification was on average 81.8%, which is in agreement with what was expected from the offline results. It should be noted that the 4-Quadrant accuracy comes from the cumulative accuracy of Lateral accuracy and '2°Q vs 3°Q' or '1°Q vs 4°Q' accuracies. That is, as it is a two-step classification, if the detected side is not correct, the quadrant is necessarily wrong. Comparing the final output of the P300, P300-Lateral, and P300-4Q detectors we observe that for participants P1 and P4 the P300 classification was improved by 15% and 5% respectively using the hybrid P300-Lateral approach. For participant P3 the P300 accuracy was already 100% with no margin for improvement, but importantly the P300-Lat kept this performance. For participant P2 the P300-Lateral accuracy was worse than the one of P300. Overall the P300-Lat approach improved the P300 detection in 2.5%. The performance of the P300-4Q approach was always worse than the P300 classification except for participant P4.

C. Discussion and Conclusion

This study investigated whether it is possible to detect the side or quadrant of the P300-speller the user is gazing at (where the target event is located), by controlling the sequence of flashing events between sides and quadrants of the paradigm layout. The goal was to detect the phase of the SSVEP elicited by the ISI side effect of the P300 visual paradigm, without altering the paradigm nor adding

TABLE I

ONLINE ACCURACY FOR LATERAL, 4Q, P300, P300-LATERAL, AND P300-4Q DETECTION.

	Lateral	4Q	P300	P300-Lat	P300-4Q
P1	95.0%	70.0%	75.0%	**90.0**%	70.0%
P2	75.00%	75.00%	85.00%	75.00%	75.00%
P3	100.0%	87.5%	100.0%	100.0%	87.5%
P4	100.0%	95.0%	90.0%	**95.0**%	**95.0**%
Average	92.50%	81.88%	87.50%	90.00%	81.88%

other forms of stimulation. Detection of phase in SSVEPs evoked by flickers coded in frequency and phase is currently a common practice in SSVEP BCIs. Here, however, the stimuli do not flicker in the same position, but instead in different spatial random positions (according to the oddball paradigm). The user is gazing the target event while stimuli flash around that area. This increases the difficulty in eliciting a SSVEP and in particular in detecting the associated phase, when compared to typical flickering stimuli, and therefore is more challenging.

The general methodological approach and in particular the SSFCB spatial filter were effective for phase detection. The offline analysis and results show that there is a clear phase discrimination between the left and right sides, but less pronounced between quadrants. By detecting the side or quadrant efficiently, the P300 target event can be selected from the smaller restricted number of events of the respective side or quadrant. An improvement of the overall P300 classification occurs whenever there is a P300 detection error and the P300 event is the one with the highest score in the detected side or quadrant. However, if the side or quadrants are misclassified, the overall classification can become worse. The online results showed that for the P300-Lateral approach, two participants improved the performance, one kept the performance (100%), and one participant got a worse performance. These results show that this approach is effective for almost all participants, but not for all. The main limitation seems to be related to a shift of the reference phase across sessions which decreases the generalization of the classification models. The P300-Quadrant approach was not effective, which is attributed to the higher variability of the measured phase. Overall, these preliminary results are promising and suggest that the P300-Lateral approach can be used effectively in some participants to improve the classification performance and reliability of the BCI. To fully validate the method, more experiments are required with a larger group, and further analysis is needed to understand the phase variability across sessions. Other approaches can be implemented combining the P300 scores with Lateral and Quadrant scores instead of the simple two-step classification presented here.

REFERENCES

[1] J. R. Wolpaw, N. Birbaumer, D. J. McFarland, G. Pfurtscheller, and T. M. Vaughan, "Braincomputer interfaces for communication and control," *Clin. Neurophys.*, vol. 113, no. 6, pp. 767 – 791, 2002.

[2] R. E. Bauer G, Gerstenbrand F, "Varieties of the locked-in syndrome," *J Neurol.*, vol. 221, no. 2, pp. 77–91, 1979.

[3] S. Barbosa, G. Pires, and U. Nunes, "Toward a reliable gaze-independent hybrid bci combining visual and natural auditory stimuli," *J. of Neurosc. Meth.*, vol. 261, pp. 47 – 61, 2016.

[4] C. Guger, R. Spataro, B. Z. Allison, A. Heilinger, R. Ortner, W. Cho, and V. La Bella, "Complete locked-in and locked-in patients: Command following assessment and communication with vibro-tactile p300 and motor imagery brain-computer interface tools," *Frontiers in Neuroscience*, vol. 11, p. 251, 2017.

[5] G. Mller-Putz, R. Leeb, M. Tangermann, J. Hhne, A. Kbler, F. Cincotti, D. Mattia, R. Rupp, K. Mller, and J. d. R. Milln, "Towards noninvasive hybrid braincomputer interfaces: Framework, practice, clinical application, and beyond," *Proc of the IEEE*, vol. 103, no. 6, pp. 926–943, June 2015.

[6] S. Sadeghi and A. a. Maleki, "Recent advances in hybrid brain-computer interface systems: A technological and quantitative review," *Basic and Clinical Neurosc. J.*, vol. 9, no. 5, 2018.

[7] M. Wang, I. Daly, B. Z. Allison, J. Jin, Y. Zhang, L. Chen, and X. Wang, "A new hybrid bci paradigm based on p300 and ssvep," *J. Neurosc. Meth.*, vol. 244, pp. 16 – 25, 2015.

[8] E. Yin, T. Zeyl, R. Saab, T. Chau, D. Hu, and Z. Zhou, "A hybrid braincomputer interface based on the fusion of p300 and ssvep scores," *IEEE Trans. on Neur. Syst. and Rehab. Eng.*, vol. 23, no. 4, pp. 693–701, July 2015.

[9] G. Pfurtscheller, B. Allison, G. Bauernfeind, C. Brunner, T. Solis Escalante, R. Scherer, T. Zander, G. Mueller-Putz, C. Neuper, and N. Birbaumer, "The hybrid bci," *Frontiers in Neuroscience*, vol. 4, p. 3, 2010.

[10] G. Pires, U. Nunes, and M. Castelo-Branco, "Comparison of a row-column speller vs a novel lateral single-character speller: assessment of bci for severe motor disabled patients," *Clin. Neurophys.*, vol. 123, no. 6, pp. 1168–1181, 2012.

[11] L. A. Farwell and E. Donchin, "Talking off the top of your head: toward a mental prosthesis utilizing event-related brain potentials," *Electroenceph. and Clin. Neurophys.*, vol. 70, no. 6, pp. 510–523, 1988.

[12] A. Cruz, G. Pires, and U. J. Nunes, "Double ErrP Detection for Automatic Error Correction in an ERP-Based BCI Speller," *IEEE Trans. on Neur. Syst. and Rehab. Eng.*, vol. 26, no. 1, pp. 26–36, 2018.

[13] C. Jia, X. Gao, B. Hong, and S. Gao, "Frequency and phase mixed coding in ssvep-based brain–computer interface," *IEEE Trans. on Biomed. Eng.*, vol. 58, no. 1, pp. 200–206, Jan 2011.

[14] G. Pires, U. Nunes, and M. Castelo-Branco, "Statistical spatial filtering for a P300-based BCI: Tests in able-bodied, and patients with cerebral palsy and amyotrophic lateral sclerosis," *J. of Neurosc. Meth.*, vol. 195, no. 2, pp. 270–281, 2011.